ISSN: 0067-2904

Adopting Image Integration Techniques to Simulate Satellite Images

Heba Khudhair Abbas*, Farah Faris, Sale Sami, Al Zahraa Fadel
University of Baghdad/College of Science for Women/ Department of Physics/Baghdad/Iraq

Received: 2/10/2019 Accepted: 18/5/2020

Abstract

Mathematical integration techniques rely on mathematical relationships such as addition, subtraction, division, and subtraction to merge images with different resolutions to achieve the best effect of the merger. In this study, a simulation is adopted to correct the geometric and radiometric distortion of satellite images based on mathematical integration techniques, including Brovey Transform (BT), Color Normalization Transform (CNT), and Multiplicative Model (MM). Also, interpolation methods, namely the nearest neighborhood, Bi-linear, and Bi-cubic were adapted to the images captured by an optical camera. The evaluation of images resulting from the integration process was performed using several types of measures; the first type depends on the determination of quality in the regions of the edges using a contrast measure as well as the number of edges and threshold. The second type is the global one that is based on the parameters of the image region, including the Mean (μ), Standard Deviation (SD), and Signal to Noise Ratio (SNR). The parameters also included the Amount of Information Added (AIA) to the original image, such as those for the total (AIA_t) , edges (AIA_e), and homogenous (AIA_h) regions. The results showed the efficiency of the integration process in the image fusion with different resolutions in one image integrated resolution. The quality measures used were also capable in evaluating the most efficient techniques and determining the accurate information of the resulting image.

Keywords: geometric distortion, mathematical integration techniques, statistical measures, interpolation method.

اعتماد تقنيات دمج الصور لمحاكاة صور الأقمار الصناعية

هبه خضير عباس* ، فرح فارس قدوري ، سلا سامي حمزه ، الزهراء فاضل عدنان
قسم الفيزياء ، كلية العلوم للبنات، جامعة بغداد، بغداد، العراق

الخلاصة

تقنيات التكامل الرياضي هي تقنيات تكامل تعتمد على العلاقات الرياضية مثل الجمع والطرح والقسمة والطرح لدمج الصور بدقة مختلفة لتحقيق أفضل تأثير للاندماج. في هذه الدراسة ، تم اعتماد محاكاة لتصحيح التشويه الهندسي والإشعاعي لصور الأقمار الصناعية بناءً على تقنيات التكامل

*Email: Physics_heba@yahoo.com

الرياضي (Brovey Transform BT) ، وتحول تطبيع اللون (CNT) والنموذج المضاعف (MM واستخدام طرق الاستيفاء) أقرب حي ، Bi–خطي و ثنائي المكعب (للصور الملتقطة بواسطة الكاميرا الضوئية. تقييم الصور الناتجة عن عملية التكامل باستخدام عدة أنواع من القياسات ؛ يعتمد النوع الأول على تحديد الجودة في مناطق الحواف باستخدام تباين مع عدد الحواف والعتبة. النوع الثاني هو النوع العالمي الذي يعتمد على منطقة الصورة (المتوسط μ والانحراف المعياري SD والإشارة إلى نسبة الضوضاء SNR وكمية المعلومات المضافة إلى إجمالي الصورة الأصلية ومنطقة الحافة والتجانس (AIAt,e,h). النتائج بينت كفاءة عملية التكامل في دمج الصورة بدرجات دقة مختلفة في صورة واحدة الدقة المتكاملة وكفاءة مقاييس الجودة في تقييم أي من التقنيات الأفضل وتحديد المعلومات الدقيقة للصورة الناتجة.

1. Introduction

The fusion of satellite images is considered as one of the topics that have been rarely addressed by Iraqi researchers due to the major obstacle of the lack of permission to utilize various satellite images taken in various wave bands for the same scene . Besides, this subject was investigated in the literature by using many different tools, leading to a difficulty in deciding the suitable approach for the interpretation of the resulted data. Due to that, this paper was produced in order to enhance the availability of base knowledge and contribute to the field of integrating satellite images [1]. Earth observation satellites offer data for different sections of the electromagnetic spectrum at different times, locations and spectral resolutions. Advanced fusion techniques of analytical or numerical data are being developed, for a full exploitation of increasingly sophisticated multisource data [2]. In fused images, data with different characteristics are combined so that increased interpretation capabilities and more reliable results are provided [3]. Since the images differ in their time, location and spectral resolution, these techniques provide the most complete view of the observed objects [4,5]. In this paper, we apply a simulation to correct the geometric and radiometric distortions that occur in satellite images due to the variety and increasing number of data that differ in attitude, scanning angle, and resolution, as well as in their temporal, spectral, spatial, radiometric distribution. Mathematical integration techniques are adopted which rely on different mathematical interpolation methods, as important and effective methods of image integration. Also, the results of the quality and efficiency of the resulting images, before and after the use of the merger, were evaluated using two types of statistical criteria to determine the accurate image information, for which the mathematical integration techniques were proven to be the most efficient.

2. Geometric and Radiometric Distortion

The engineering relationships between the location of the entry pixel (column and row) and the map coordinates associated with the same point (x, y) must be determined. This will determine the nature of the conversion of geometric coordinates that have been applied to correct or move each pixel in the original input image (x 'and y') to its correct position in the corrected output image (x, y). This process was advocated for spatial interpolation [6].

Geometric distortions can be separated into two groups: systematic or predictable and sensor-related distortions. Systematic and consistent distortions that can be corrected by calibration are called internal, random, or unexpected distortions that occur due to platform disturbances and landscape characteristics and change by nature [7]. These distortions can be identified from the elevation model and in some cases from the Digital Terrain Model (DTM) or from the control points taken on the images and called external [8].

Radiometric distortion the pixels in the corrected output image required a valuable of grid about entry pixels which is not falling roughly on a (row - and column) coordinates [9]. When this occurs, there must be a mechanism to determine the brightening value that has been allocated to the new modified pixel; this process is known as intensity of interpolation [10]. Radiation distortions are characterized by incorrect density distortion, spatial frequency filtering of scene data, discoloration of the image, an image data range, and so on. These distortions are caused by camera or scanner shading effects, reagent gain changes, atmospheric changes, and induced a sensor. Filtering, sensor defects, sensor detector gain errors, etc. They can also be separated into two types: systematic or predictable and random or unexpected.

3. Interpolation Methods

Interpolation is a process of calculating an unknown value from a well-known value. Commonly used interpolation methods include [11]:

- Nearest neighborhood interpolation: the nearest neighbor is the simplest processing time for all interpolation algorithms. In this way, we find the closest matching pixel in the original image for each pixel in a facing image. New pixels are created by duplicating pixels or color points to create new pixels as the image grows. Pixels that divide curves are generated into steps or rough edges [12].
- Bi-linear method: The internal completion of four pixels is the closest linear for deriving the desired pixel. Bi-linear is considered a delicate technique compared to the nearest neighborhood interpolation. Suppose that (x, y) are the coordinates of the location and the pixel intensity is v (x, y). Bi-linear completion gives more accurate results than the nearest interpolation of neighbors, with an increase in calculations [13].
- Bi-linear interpolation: One of the most complex processes to some extent linear bilateral completion. In bi-cubic interpolation, caret and have to rely on the sixteen nearest neighbors of pixels. This method is one of the best ways to maintain the accuracy of the details in a manner that is more efficient than bilateral interpolation [11].

4. Mathematical Integration Techniques

Using simple calculations to merge two or more images, these techniques assume that there is a high correlation between the first and each of the second bands. Some of the popular techniques of this type include the BT, CNT and MM, as described below [10].

4.1 Brovey Transformation (BT)

Brovey transformation is a relative method by which data values for each range of first image data (I1) are divided by the sum of the data of I1 and multiplied by the second image data set (I2). Brovey transformation attempts to maintain the spectral line of each linear integrity band, by adding the proportional value of each band according to the I1 data before combining it with the I2 dataset. By adjusting the effects of the spectral properties of the I2 data collected, the spectral quality of this group is maintained in the I1 data [14], as described by the following relation:

$$BT_{i,j,k} = \frac{I_{1_{i,j,k}}}{\sum_u I_{1_{i,j,u}}} \times I_{2_{i,j}} \quad ,\ldots\ldots (1)$$

where $BT_{i,j,k}$ is the output image, i and j are pixel coordinates , k is the band index, and u is the summation bands I_1 . The Brovey increase in optical contrast at the graphic image has given this property a noticeable development. As a result, it is preferable to use the Brovey converter when the state of maintaining the original radiation measurement is necessary. However, an RGB image is produced with high contrast technology from the high and low sides of the graph images [14].

4.2 Color Normalized Transform (CNT)

The color normalized transformation fuses the two spectral and spatial datasets assuming that there is a certain spectral overlap between the first image (I_1) domains and the second image (I_2) domains which are more highly resolved. These constrains are breached for the close IR domain, which leads to a weak fusion outcome. Eq. (2) describes the merge operation. This method is an improvement of Brovey method, in which the images contain high color distortion, by adding some values so that the result of division is not equal to zero [14]:

$$CNT_{i,j,k} = \frac{3*\left(I_{1_{i,j,k}}^{low}+1\right)\left(I_2{}^{high}+1\right)}{\sum_{s,t} I_{1_{s,t,k}}^{low}+3} \quad ,\ldots\ldots\ldots\ldots (2)$$

4.3 Multiplicative Model (MM)

The multiplication algorithm is derived by four mathematical methods (addition, subtraction, division and multiplication). It combines an intense image into a color image where multiplication represents a low probability of color distortion. The multiplier model collects two datasets and compensates for the increase in BV by taking a square root of a set of merged data. It illustrates the mixed spectral characteristics of both groups, as follows [14,15]:

$$MM_{i,j,k} = \sqrt{I_{1_{i,j}} \times I_{1_{i,j,k}}} \quad ,\ldots\ldots\ldots\ldots (3)$$

5. Quality Assessment Measures

The results were evaluated by image quality criteria because the images applied in this research contain any color and modern information. As a result two types of image quality standards were obtained, which are the quality standards proposed in this study variance and the number of edge points for different threshold and traditional quality standards (SD, SNR, AIAt, AIAe, and AIAh). Using the color change criterion, the quality of color information can be measured to calculate the quality of color information [10].

6. Practical parts and algorithms

The study included the following several parts.

i. Capturing a pair of visual images using digital camera, one color image, image balloon size (128×108) pixels, and bit depth of 24 bits. Each bundle has values between 0-255.The other image is a grayscale image with balloon size of 256×215 pixels, bit depth of 8 bits), and gray levels of intensity ranging between 0-255, as shown in Figure-1.

(a) (b)

Figure 1 (a, b)- Visual images captured

ii. Using MATLAB (2017R) to build and develop algorithms.

iii. Results of mathematical mergers

This part shows the results of merging by the mathematical techniques (BT, CNT and MM), which involved the following steps:

Step 1: Read color image (A) and display;

Step 2: Convert RGB image (A) grayscale: I=rgb2gray (A);

Step 3: Resize image: B = imresize (A, scale) where scale (0.3, 0.5, 0.25, 0.0625 and 0.025);

Step 4: resize image by the interpolation A=imresize (A, Scale, method); where the methods are (nearest, Bi-linear and Bi-cubic)

Step 5: Compute three color bands (RGB) for color image; R=im1; G=im2; B=im3;

Step 6: Compute Brovey merge equation:

immerge_ BT=C. /ss

where ss=double (im1) +double (im2) +double (im3) and C =A*I;

Step7: Compute CNT merge equation:

immerge_CNT= (C. /ss+3)-1; where C= (A+1).*(I+1))*3;

Step8: Compute MM merge equation:

immerge_MLT= sqrt (double(C); where C= (A+1).*I;

Step 9: end steps

The results of the use of this merger are shown in Figure-2.

- **BT results**

Rs=0.5 Rs=0.3 Rs=0.25 Rs=0.0625 Rs=0.025

a: nearest method

Rs=0.5 Rs=0.3 Rs=0.25 Rs=0.0625 Rs=0.025

b: Bi-linear method

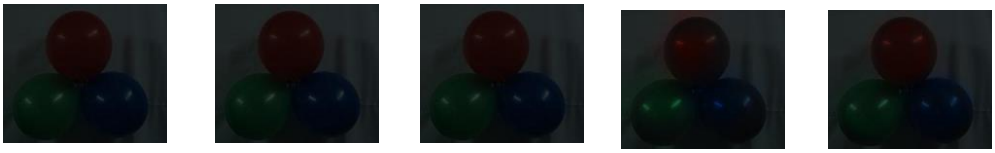

Rs=0.5 Rs=0.3 Rs=0.25 Rs=0.0625 Rs=0.025

c: Bi-cubic method

CNT results

Rs=0.5 Rs=0.3 Rs=0.25 Rs=0.0625 Rs=0.025

a: nearest method
Continuo Figure-2

Rs=0.5 Rs=0.3 Rs=0.25 Rs=0.0625 Rs=0.025

b: Bi-linear method

Rs=0.5 Rs=0.3 Rs=0.25 Rs=0.0625 Rs=0.025

c: Bi-cubic method
Continuo Figure-2

MM results

Rs=0.5 Rs=0.3 Rs=0.25 Rs=0.0625 Rs=0.025

a: nearest method

Rs=0.5 Rs=0.3 Rs=0.25 Rs=0.0625 Rs=0.025

b: Bi-linear method

Rs=0.5 Rs=0.3 Rs=0.25 Rs=0.0625 Rs=0.025

c: Bi-cubic method

Continuo Figure-2

iv. Quality Assessment Results

The quality of the evolution of the output that resulted from merging images is assessed by using several quality measures. These measures can be classified into two types; the first is based on determining the quality in image edge regions (contrast calculation with the number of edges and threshold). The second is the global measures that are based on image region (μ, SD, SNR, and AIAt, e,h). Figure (3) shows the relation between statistical measures with resize image (RS) merge for each interpolation method adopted.

- Results of measures based on image region

a: BT results

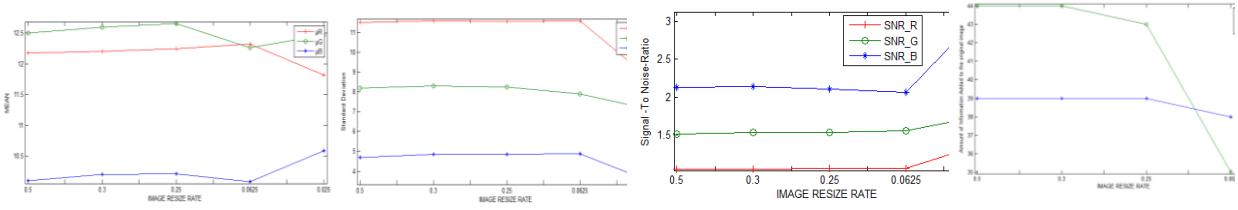

a: Nearest method

μwith RS SD with RS SNR with RS AIA $_{h,e,t}$with

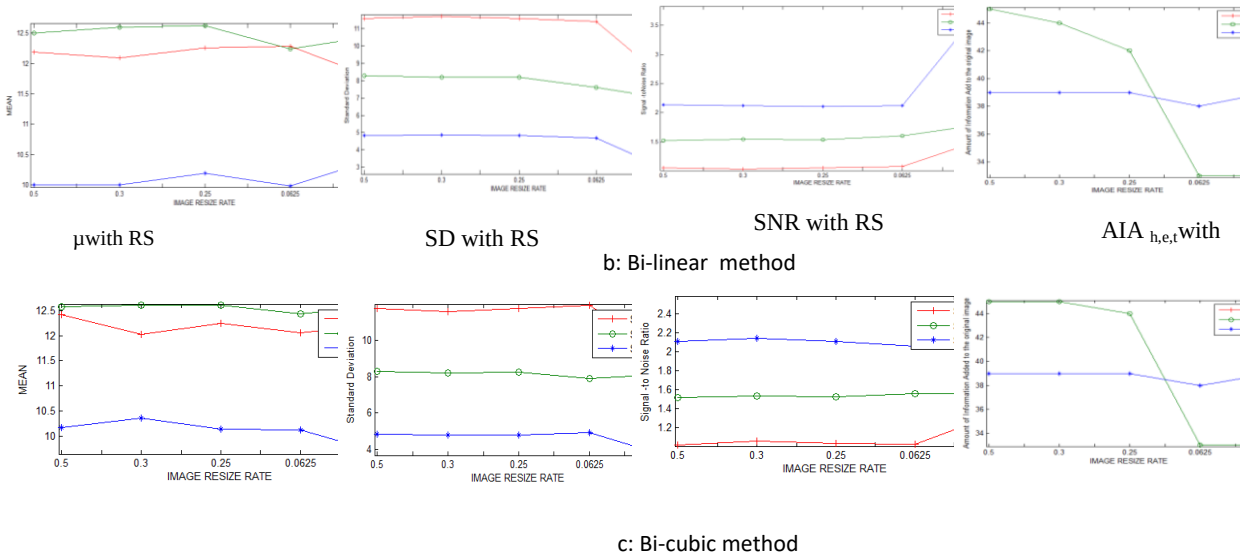

Figure 3-Relation between statistical measures with resize image (RS) merge for each interpolation method adopted

From Figure-3, several observations can be noticed. Bu using the Nearest and Bi-linear methods, the relation between the mean and SD of the resize (RS) value was approximately constant for all color bands (RGB), except for a clear reduction in resize values for mean (0.0625) and SD (0.025), indicating a low amount of information of any distortion at that size. However, SNR value after RS was approximately constant for all color bands , except for being clearly high when the RS was (0.025), which indicates the existence of homogeneous regions at that size. As for the amount of information added to the original image following image resize, the values were converged and constant for the total and homogeneous regions (AIA_t, AIA_h) and became lower with RS values of (0.0625 and 0.025). The values of edges were very high and nearly constant for all sizes, except for low sizes (0.0625).Inn addition, the Bi-cubic method showed constant relations between the values of mean, SD, SNR and $AIA_{t,h,e}$ following SR for all color bands . However, there was a clear increase which was higher than that observed using the two previous methods (nearest & Bi-linear). In addition, the value of SNR was lower than that for these two previous methods.

b: CNT results

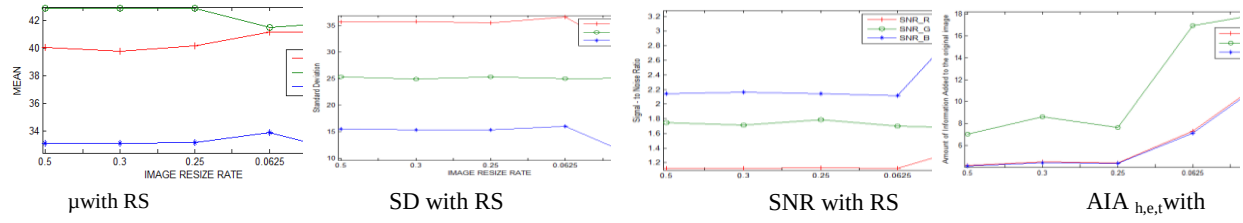

c:MM results

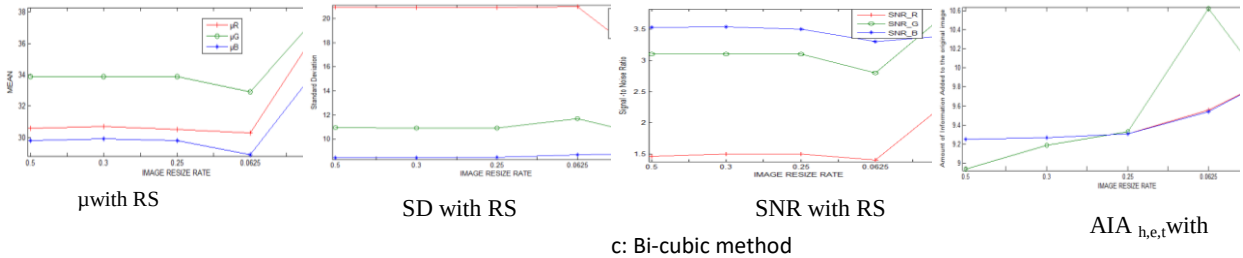

Continuo **Figure-3**

From Figure 3b and c,, the results of merging the CNT and MM methods indicated that Bi-cubic interpolation method produced the highest quality.

In figure (3b), it is noticed that the mean value was approximately constant for all color bands except for a clear reduction in the size (0.0625). SD value was approximately constant for the green band, with a clear reduction in (RB) bands at RS of (0.025). In addition, SNR value was approximately constant in all color bands except for highly clear with RS of (0.025). AIA values were converged and constant for the $AIA_{t,}$ AIAh and AIA_e regions, except for an increase at RS values of (0.0625 and 0.025).

In figure (3c), it is observed that the mean value was approximately constant for all color bands, except for a clearly low value when the RS was (0.0625), then a high value at RS of (0.025). The SD value was approximately constant for all (RGB) bands, except for a clear reduction in (R) band at RS of (0.025). SNR value was approximately constant for all RGB bands, except a for a clearly high value in (RG) bands when the TS was (0.025). The values of the AIA to the original image following image resize were converged and constant for the AIA_t and AIA_h regions, except for clearly high values at RS of (0.0625 and 0.025). However, AIA_e value increased linearly for all RS values, except at (0.0625) where a clear increase, then a reduction, at RS of (0.025).

- Results of measures based on determining the quality in image edge regions (contrast calculate with number of edges and threshold)

When the Sobel's detector was applied to each merge resize image (BT,CNT and MM) accredited integration to take ten different threshold values by each image and measure the statistical contrast, and the best results are shown using interpolation methods adopted results as shown the best contrast in Bi-cubic interpolation in Figure-4.

a: BT results

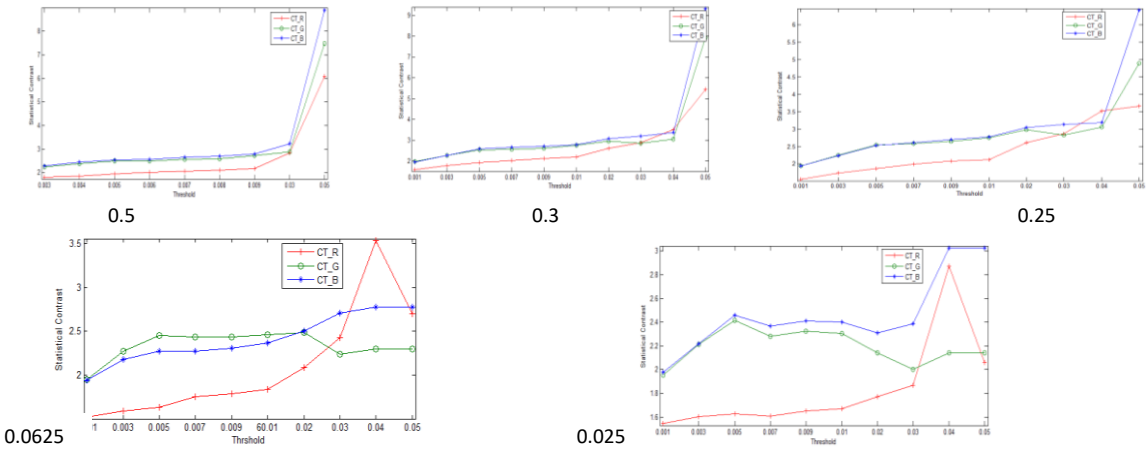

0.5 0.3 0.25

0.0625 0.025

b: CNT results

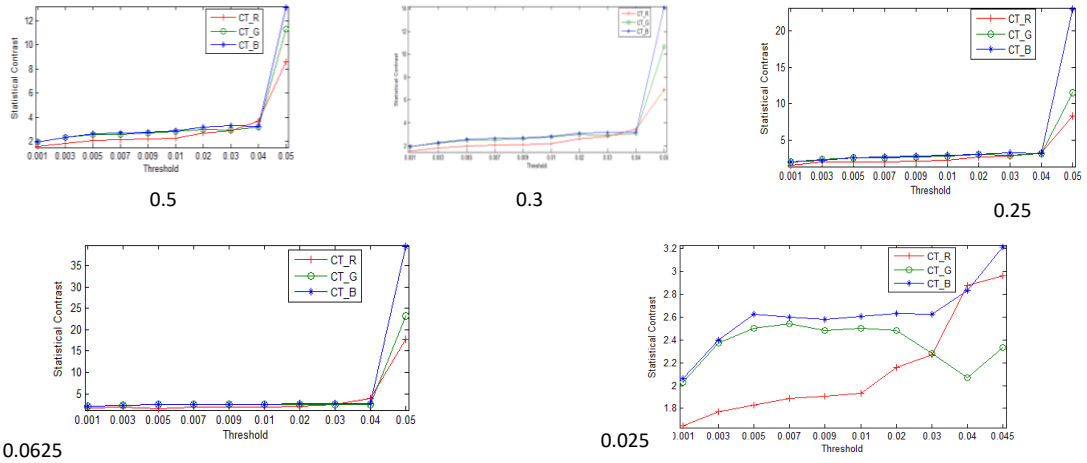

0.5 0.3 0.25

0.0625 0.025

c: MM results

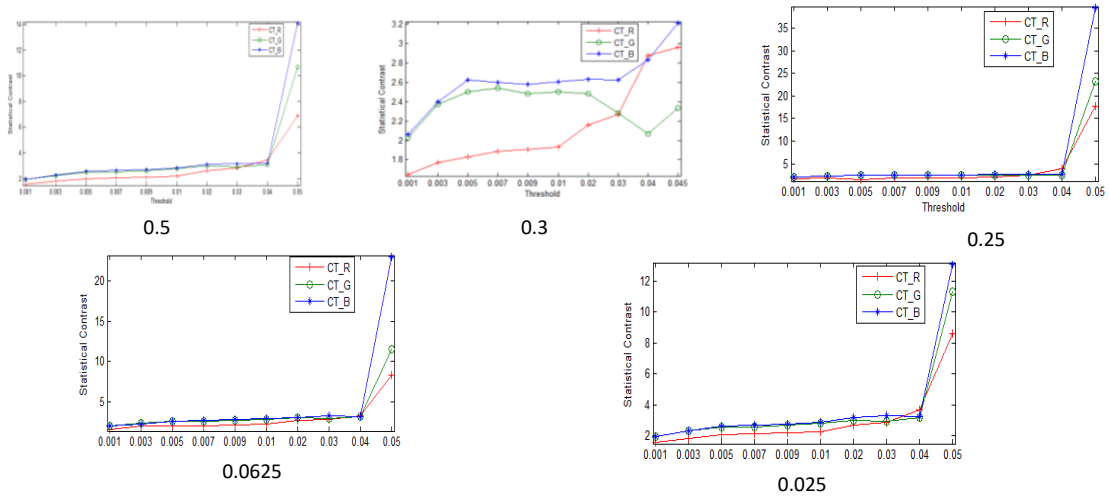

Figure 2-Relations between contrasts with threshold of Bi-cubic interpolation image for each resized fused image

• Results of quality measures represented number of edges points with threshold for each interpolation methods adopted here applied Sobel's detector to each fused image to evaluate the quality the details of those images resulting from the integration techniques (BT,CNE and MM), especially the edge detected, the results were shown from Table-(1a,b and c).

Table 1-Relations between numbers of edge points with different threshold values using Bi-cubic interpolation method

a: BT

RS=0.5		RS=0.3	RS=0.25	RS=0.0625	RS=0.025
Th	No.of edges	No.of edges	No.of edges	No.of edges	No.of edges
0.001	11602	11513	11559	11712	11414
0.003	5353	5471	5420	5378	5180
0.005	2546	2566	2525	2539	2425
0.007	1521	1548	1553	1502	1525
0.009	1113	1114	1136	1117	1116
0.01	980	970	976	985	975
0.02	552	557	559	567	579
0.03	299	298	301	282	279
0.04	77	76	80	63	58
0.05	7	7	5	1	1

b: CNT

RS=0.5		RS=0.3	RS=0.25	RS=0.0625	RS=0.025
Th	No.of edges	No.of edges	No.of edges	No.of edges	No.of edges
0.003	11123	11173	11035	11080	11242
0.005	7919	7865	7830	8005	7937
0.007	5825	5784	5823	5895	5889
0.009	4506	4499	4557	4529	4548
0.03	920	916	918	917	923
0.05	718	712	710	713	720

0.07	525	526	528	531	536
0.09	370	364	367	352	348
0.1	256	260	260	254	243
0.15	11	13	12	6	7

c: MM

RS=0.5		RS=0.3	RS=0.25	RS=0.0625		RS=0.025
Th	No.of edges	No.of edges	No.of edges	Th	No.of edges	No.of edges
0.003	10661	10208	10333	0.001	14399	14829
0.005	7412	6940	7050	0.002	12522	9932
0.007	5413	5019	5134	0.003	10463	6008
0.009	4171	3862	3878	0.005	7034	3877
0.03	855	842	854	0.007	8474	2665
0.05	645	539	518	0.009	3376	2089
0.07	462	295	254	0.03	603	580
0.09	248	91	37	0.05	221	203
0.1	146	32	14	0.07	34	20
0.13	14	9	3	0.09	1	5

From the results in Table-1, it is noticed that the best values were obtained by using the Bi-cubic interpolation. It is observed that the number of edge points decreases when the threshold value increases.

8. Conclusions

The process of integrating images is important in remote sensing and geographic systems, as it works to integrate different information and data taken from different sensors in one image containing all the spectral and spatial information. This process is similar to the process of registring images of satellites, called geometric correction, which represents a comparison of data captured at different times on a point-by-point basis. According to the results, it was noticed that the best results were obtained by using the Bi-cubic method, based on the efficiency and quality of statistical measures adopted in the evaluation and examination of the quality of images resulting from the process of integration.

9. References

1. Lucien W., Thierry R. and Marc M. **1997**. "Fusion of satellite images of different spatial resolutions: Assessing the quality of resulting images", Photogrammetric engineering and remote sensing, *Asprs American Society for Photogrammetric*, **63**(6): 691-699.
2. M. Gašparović, , D. Medak and et al, **2018** , "Fusion Of Sentinel-2 And Planetscope Imagery For Vegetation Detection And Monitoring", The International Archives of the Photogrammetry, Remote Sensing and Spatial Information Sciences, Volume XLII-1, ISPRS TC I Mid-term Symposium "Innovative Sensing – From Sensors to Methods and Applications", 10–12 October 2018, Karlsruhe, Germany.
3. Mc. Cabe, M. F., Aragon and et al, **2017**, CubeSats in Hydrology: Ultrahigh-Resolution Insights into Vegetation Dynamics and Terrestrial Evaporation. *Water Resources Research*, **53**(12): 10017-10024.
4. Houborg, R., and McCabe, M.F., **2018**, Daily Retrieval of NDVI and LAI at 3 m Resolution via the Fusion of CubeSat, Landsat, and MODIS Data. *Remote Sensing*, **10**(6): 890.
5. Hermosilla, T., Wulder, M.A., and et al, 2015. Regional detection, characterization, and attribution of annual forest change from 1984 to 2012 using Landsat-derived time-series metrics. *Remote Sensing of Environment*, **170**: 121-132.

6. Traganos, D., Cerra, D., and Reinartz, P. **2017**. CubeSat-derived detection of seagrasses using Planet imagery following Unmixing-based Denoising: is small the next big?. In: The International Archives of the Photogrammetry, *Remote Sensing and Spatial Information Sciences*, **XLII**(1/W1): 283- 287.
7. Heba Kh. **2013**. "A study of digital image fusion techniques based on contrast and correlation measures", thesis PhD. Al Mustansiriah university, college of science.
8. H.Ghassemian. **2016**."A review of remote sensing image fusion methods", ELSEVER *Information Fusion*, **32**(Part A): 75-89.
9. Jensen R.J, **1968**. "Introductory Digital Image Processing", 2nd,Prentice Hall, New Jersey, 1986.
10. Starck J.L, Murtagh F, Bijaoui A. **1998.** "*Image Processing and Data Analysis: The Multi scale Approach* ", Cambridge University Press, 1998.
11. Dong J., Zhuang D., Huang Y., Jingying Fu. **2009**. "Advances in Multi-Sensor Data Fusion: Algorithms and Applications ". Review, ISSN 1424-8220 Sensors, 9, pp.7771-7784.
12. Zhang J., **2010**. "Multi-source remote sensing data fusion: status and trends", *International Journal of Image and Data Fusion*, **1**(1): 5–24.
13. Heba, Kh. Abbas, Ali, A.D. and Anwar H. M., **2014**. "Multifocus Images Fusion Based On Homogeneity and Edges Measures*". Journal Baghdad for Science*, **11**(2): 661-663.
14. Heba Kh. Abbas, Anwar H. and Ali A., **2109**. " Optical Images Fusion Based on Linear Interpolation Methods", Iraqi Journal of Science, 2019, **60**(4): 924-936.
DOI: 10.24996/ijs.2019.60.4.26.
15. Hebe Kh. Abbas, Sally F. Ahmed and Anwar H., **2017**. "Quantitative Analysis based on Supervised Classification of Medical Image Fusion Techniques", *Iraqi Journal of Science*, **58**(3B): 1546-1554, DOI: 10.24996/ ijs.2017.58.3B.19